Understanding the Effects of PEMFC Contamination from Balance of Plant Assembly Aids Materials: In Situ Studies

Md. Opu,[a,b,d] G. Bender,[b,*] Clay S. Macomber,[b] J. W. Van Zee,[a,c,*] and Huyen N. Dinh[b,*,z]

[a]*Department of Chemical Engineering, University of South Carolina, Columbia, South Carolina 29208, USA*
[b]*National Renewable Energy Laboratory (NREL), Golden, Colorado 80401, USA*
[c]*Department of Chemical and Biological Engineering, University of Alabama, Tuscaloosa, Alabama 35487-0203, USA*

In situ performance data were measured to assess the degree of contamination from leachates of five families of balance of plant (BOP) materials (i.e., 2-part adhesive, grease, thread lock/seal, silicone adhesive/seal and urethane adhesive/seal) broadly classified as assembly aids that may be used as adhesives and lubricants in polymer electrolyte membrane fuel cell (PEMFC) systems. Leachate solutions, derived from soaking the materials in deionized (DI) water at elevated temperature, were infused into the fuel cell to determine the effect of the leachates on fuel cell performance. During the contamination phase of the experiments, leachate solution was introduced through a nebulizer into the cathode feed stream of a 50 cm^2 PEMFC operating at 0.2 A/cm^2 at 80°C and 32%RH. Voltage loss and high frequency resistance (HFR) were measured as a function of time and electrochemical surface area (ECA) before and after contamination were compared. Two procedures of recovery, one self-induced recovery with DI water and one driven recovery through cyclic voltammetry (CV) were investigated. Performance results measured before and after contamination and after CV recovery are compared and discussed.
© The Author(s) 2015. Published by ECS. This is an open access article distributed under the terms of the Creative Commons Attribution 4.0 License (CC BY, http://creativecommons.org/licenses/by/4.0/), which permits unrestricted reuse of the work in any medium, provided the original work is properly cited. [DOI: 10.1149/2.0411509jes] All rights reserved.

Manuscript submitted April 3, 2015; revised manuscript received May 28, 2015. Published June 29, 2015. This was Paper 1293 presented at the Honolulu, Hawaii, Meeting of the Society, October 7–12, 2012.

While the energy conversion efficiency of proton exchange membrane fuel cell (PEMFC) systems is relatively high, economical applications have been limited due to initial stack costs and the degradation of performance over time which can be affected by contaminants that enter the system with the air or fuel feed stream, or component materials of construction leaching into the gas/water stream.[1–12] Present-day requirements for durability limit the performance loss to 80 mV over required lifetimes of 5000 hours. Since potential cycling, start/stop, and idling conditions contribute to these performance losses,[11,13–15] the tolerance for losses due to contamination is much smaller than 80 mV. In addition, with the recent reduction in cost related to the fuel cell stack, the relative cost of balance of plant has risen. This presents the opportunity to further reduce overall system cost by choosing functional, low cost BOP materials for PEMFC systems. Educated selection of BOP materials requires a level of understanding of potential contaminants from system components that does not currently exist in the literature. Chemically inert and low cost materials with low amounts of total and non-reactive leachates would be the most desirable materials for fuel cell applications.[16] This paper focuses on the effect of leachates from system components on fuel cell performance and seeks to add to the limited knowledge base discussing PEMFC contaminants from system components.[2,3,5,7–9,12,17–24]

Here we describe (1) a protocol to create leachate solutions from BOP materials, (2) ex situ quantification and speciation of the components present in the BOP leachate solutions, (3) in situ quantification of performance effect due to the leachate solutions and, (4) an attempt to correlate ex situ with in situ results. In our study, we are investigating commercially available commodity materials. These materials are generally developed for other applications and they may contain additives/processing aids which may be detrimental to fuel cells performance and/or durability. The information obtained will be valuable to identify low cost assembly aids BOP materials that can fulfill their function without sacrificing performance.

Experimental

This section is divided into four subsections that represent the experimental procedures performed in this work.

Leachate solution.— The leaching protocol was carried out using triply rinsed and capped polypropylene bottles. The assembly aids chosen are flowable materials which were spread out and allowed to cure on clean Teflon sheets. They were then peeled off the sheets when possible and placed in clean bottles of fresh DI water. A material surface area to volume of water ratio of 150 mm^2 / 1 ml was maintained for all samples. All bottles along with control blanks were placed in a calibrated oven at 90°C for 1 week. The exception was the Krytox lubricants, which were treated for 6 weeks due to their extremely low total organic carbon (TOC) and total inductively coupled plasma optical emission spectroscopy (ICP-OES) counts after the first week. Afterwards, the extract solutions were promptly removed and the solutions decanted off into clean bottles. This step separated the assembly aid from its leachant solution, to prevent any further leaching or re-adsorption. The conductivity of the leachate solutions were measured using a properly calibrated Thermo Orion 550 A conductivity meter.

Ex situ quantification and speciation.— All analytical experiments and analysis were described previously.[6] Gas chromatography-mass spectrometry (GCMS) was performed by a Thermo Scientific Trace/ISQ GCMS. 1.0 μl of liquid was injected into a SSL injector, volatilized and separated on a Thermo TG-5SILMS column with the resulting chromatogram generated by a total ion current [TIC] detector. The mass spectrometer was auto-calibrated to a perfluorotributylamine standard and each resulting peak/mass spectra underwent a NIST library spectral search of over 200,000+ molecules. High quality hits manually determined by the operator were reported as the species identified. After determination of model compounds selected for further study, pure standards were purchased from Sigma-Aldrich and run under the same conditions to verify molecular identification via comparison of retention time [RT] and mass spectrum.

TOC was measured with General Electric [GE] Innovox and TOC 900 instruments. Calibration standards were made from pure sucrose and multiple trials were run and averaged for reproducibility.

ICP-OES was performed using a Perkin Elmer Optima 5300 DV axial radial instrument with a segmented array charge coupled device [SCD] and a shear gas of argon. Samples were acidified using nitric acid and the system was calibrated for 29 different ions before and after runs. The ICP total value was calculated as the sum of the twenty nine individual values and is reported in Figure 1.

*Electrochemical Society Active Member.
[d]Present Address: Oorja Fuel Cells, Fremont, California 94539, USA
[z]E-mail: Huyen.dinh@nrel.gov

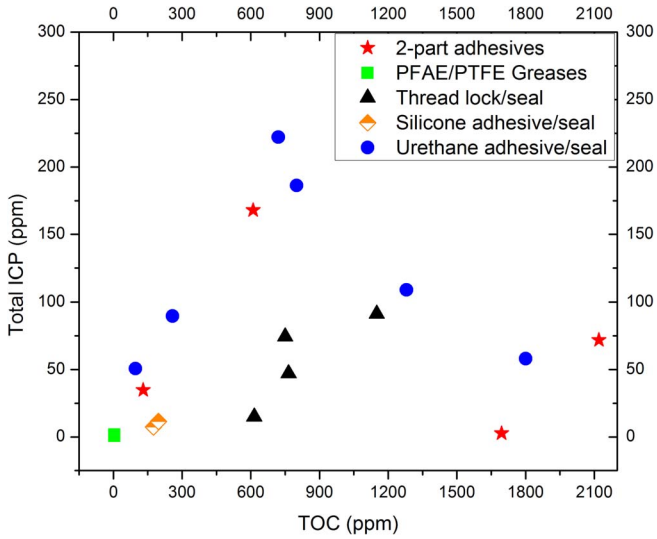

Figure 1. Relation between total ICP and total TOC. All families except the PAFE/PTFE greases were soaked for 1 week in DI water at 90°C. The PFAE/PTFE greases materials were soaked for 6 weeks due to their inherent cleanliness and lack of leachates.

In situ quantification of performance effect.— All of the data reported here were obtained with membrane electrode assemblies (MEAs) prepared by General Motors Electrochemical Energy Research Lab. They contained a DuPont Nafion 211 membrane, a 0.05 mg/cm^2 Pt/C (Tanaka carbon) loading on the anode, and a 0.4 mg/cm^2 Pt/C (Tanaka carbon) loading on the cathode side. DuPont D2020 ionomer was used in the preparation of the catalyst inks and 3M MRC 105 diffusion media were used for the gas diffusion layer. The active area of the MEAs was 50 cm^2. All MEAs were conditioned using a load cycling procedure that included cycling between very low and increasingly higher current densities for several hours.

A commonly used single cell hardware design was used that employed endplates, current collector plates, and graphite flow-fields. The hardware was assembled using a torque of 4.52 Nm on each of the eight bolts. The anode/cathode flow-fields consisted of two/three channel serpentine designs, respectively. Prior to operation the assembled hardware, with the MEAs were tested for leaks.

In situ testing was performed on a Model 850 e test station (Scribner Associates Inc.). The test station was calibrated with respect to temperatures, gas flows, gas humidities, and pressures. High purity hydrogen and industrial grade compressed air was used as the fuel and reactant. For all experiments, the temperature of the cell was controlled using a heating/cooling strategy with cartridge rods and a fan.

Polarization experimental.—Standard operating conditions (SOC) for polarization experiments were 80°C cell temperature, stoichiometric flow rates of 1.5/2, and backpressures of 150/150 kPa, for anode/cathode respectively. Experiments were performed at two different relative humidity settings: 32/32% RH and 100/100% RH. These conditions will be referred to as 'dry' and 'wet', respectively. To perform a polarization experiment, the cell current density was first reduced from 1.5 A/cm^2, to open circuit in seven steps (1.5, 1.2, 1.0, 0.8, 0.4, 0.2, 0.05, 0 A/cm^2) then increased again using the same steps. Sufficient time of 15 minutes between changes in the current resulted in no observed hysteresis in the polarization curves.

Infusion Test.—After conditioning, beginning of test (BOT) diagnostics were performed on the MEA. These included, in chronological order, a dry and a wet polarization curve, and cyclic voltammetry experiments for both the cathode and the anode electrodes. Conditions for the CV experiments were: 25°C (room temperature) cell temperature, 200/100 sccm H_2/N_2 flow rates, 100/100% RH, and 100/100 kPa backpressures. The applied potential ranged from 0.04 to 1.05 or 1.1 V vs the hydrogen electrode (HE). The third scans of the CV experiments were used to calculate the electrochemically active surface areas (ECAs) of the electrodes.

Following BOT diagnostics, the setup was altered to allow the cathode feed stream to be humidified via liquid injection. The gas flows were interrupted and a microflow nebulizer (Elemental Scientific) was connected to the cathode feed stream at the gas inlet of the cell. This micro-nebulizer together with a micro-flow peristaltic pump enabled the setup to deliver DI-water or leachate solution to the cell in an aerosol form. Whenever the nebulizer was used for the infusion experiment, the cathode humidifier bottle in the station was bypassed. The infusion experiment operating conditions (IEOC) were: 80°C cell temperature, a constant current of 0.2 A/cm^2, 2.0/2.0 stoichiometric flow rates, 32%/32% RH, and 150/150 kPa backpressure for anode/cathode, respectively. To create the cathode humidity conditions, a pump rate of 0.03 ml/min was used for both DI-water and leachate solution.

The injection setup was used first with DI-water and IEOC until the cell voltage had stabilized for at least 3 hours. The source bottle for the DI-water bottle was then manually switched to a bottle containing leachate solution. Since the tubing lines were not flushed the switching created a plug-flow dead time of approximately 45 min based on tube diameter and length. After 12–14 hours of infusion of leachate solution, the source bottle was switched to DI-water again and the experiment continued for approximately 3–5 hours to determine if any self-induced recovery may occur, i.e. if any cell voltage loss may recover without contaminant in the feed stream of the cathode. Cell voltage and high frequency resistance (HFR) were recorded continuously throughout the experiment.

After self-induced recovery, the setup was returned to its original state. During this change the cell potential was at open circuit potential. End of test (EOT) diagnostics were then performed to quantify the effect of the contamination on performance and durability of the MEA. EOT diagnostics were identical to BOT diagnostics with the exception that partial CVs were performed prior to the first set of polarization curves. The applied potential for the partial CV ranged from 0.04 – 0.5 V vs HE. The dry polarization curve was run before the wet curve in an effort to minimize any dilution of contaminant during the wet curve. Subsequent to EOT diagnostics dry and wet polarization curves were repeated once more to quantify any additional performance recovery induced by driving the cell potential during the CV experiments and potentially oxidizing adsorbed contaminant species.

Results and Discussion

The 20 selected assembly aids materials were grouped into five categories based on their intended use and chemical composition, as shown in Table I. The materials, while not exclusive, cover a wide range of functions and properties of typical adhesives and lubricants, and they may have various degrees of stability in water at fuel cell operating conditions. Our selection of representative system materials is based on properties such as the exposed surface area of the material that is wetted by the gas, total mass or volume in a system, function, cost, and stability in a fuel cell environment, i.e., 0% to 100% relative humidity, −40°C to 90°C. Material selection is also based on the materials' physical properties, commercial availability, and input from original equipment manufacturers and fuel cell system manufacturers. The 2-part adhesives (mostly epoxies) are used to permanently adhere two surfaces together. The perfluoroalkylether/polytetrafluoroethylene (PFAE/PTFE) greases were chosen for their superior clean lubricating properties. The thread lock/seal materials (mostly polyethylene glycol dimethacrylate [PGDMA]) are used to keep bolts tight during long-term vibration. The silicone and urethane adhesives and seals are materials that connect two materials together, close potentially larger gaps, provide a wet seal and withstand some vibrational stress.

Figure 1 summarizes the total ICP and TOC data for all materials studied. Figure 1 shows that the leachates of the materials selected cover a wide range of elemental and organic concentrations. Total ICP

Table I. TOC, Total ICP and calculated minimum % proton sites available in membrane based on total ICP for twenty assembly aids materials, grouped by chemical description and intended use.[6]

Chemical Description	Manufacturer	Trade name and use	Grade	TOC (ppm)	Total ICP (ppm)	Estimated min. fraction (%) of protons available in membrane[a] post infusion
Epoxy-Polyamide	3M	Scotch Weld 2-part Adhesive	1838 green	130	35	88
Acrylic Adhesive	LORD	LORD 2-part Adhesive	204/19 extra thick acrylic	610	168	43
Epoxy	Reltek	Bond-IT 2-part Adhesive	B45	1695	3	99
Epoxy	Reltek	Bond-IT 2-part Adhesive	B45TH	2120	72	75
PFAE/PTFE	DuPont	Krytox Grease	XHT-SX	4.4	0.7	100
PFAE/PTFE	DuPont	Krytox Grease	GPL-206	4.4	1	100
PFAE/PTFE	DuPont	Krytox Grease	GPL-207	4.2	1	100
PFAE/PTFE	DuPont	Krytox Grease	XHT-S	4.4	2	99
PGDMA	Henkel	Loctite Thread Lock/Seal	#565	615	15	95
PGDMA	Henkel	Loctite Thread Lock/Seal	#567	750	74	75
PGDMA	Henkel	Loctite Thread Lock/Seal	#577	765	47	84
Modified Resin	Henkel	Loctite Thread Seal	#80724	1150	91	69
Silicone	3M	Super Silicone Adhesive/Seal	#8663 clear	175	7	97
Silicone	3M	Super Silicone Adhesive/Seal	#8664 black	197	12	96
Urethane	Bostik	Marine Adhesive/Seal	920 Fast set	96.4	51	83
Urethane	Henkel	Loctite Adhesive/Seal	#39916	258	90	69
Urethane	3M	Marine Adhesive/Seal	5200 standard cure black	720	222	24
Urethane	3M	Marine Adhesive/Seal	5200 standard cure white	800	186	37
Urethane	3M	Marine Adhesive/Seal	4000 fast cure white	1280	109	63
Urethane	3M	Marine Adhesive/Seal	5200 fast cure white	1800	58	80

[a]Assume all species from total ICP value acted as Na^+ and all of the Na^+ ion-exchanged with the protons in the membrane. A sample calculation is shown in Appendix.

represents the summation of the elements measured in solutions. We assume that total ICP represents the inorganic ions in solution and thus it directly relates to solution conductivity. TOC represents the organics in solution. Figure 1 does not show a correlation between total ICP and TOC, as expected. The desirable BOP material for fuel cell application would ideally have low TOC and low ICP. Materials that leach less organic and/or inorganic compounds inherently have less impact on fuel cell performance. Typically higher cost materials like the selected PFAE/PTFE greases are cleaner, which is reflected in very low measured ICP and TOC values (Figure 1). Other materials like lower cost 2-part adhesives leached out more organic compounds and urethane adhesives/seals leached out more inorganic contaminants. These materials produced color changes to the solutions. Based on this ex situ screening, these materials were expected to have an impact on fuel cell performance. We would like to note that the materials were selected intentionally to have a wide range of material leachate species and levels so that the impact on fuel cell performance can be better investigated and understood.

Organic and inorganic compounds were identified via GCMS and ICP-OES conducted and reported previously on the same leachate solutions.[6] Organics observed included aldehydes, alcohols, glycols, amines and amides.[6] Inorganics observed included Na, Si, K, Mg, Ca, and S.[6] Some of the metals identified by ICP-OES analysis may be cations and they may react with the sulfonate group in the membrane and the ionomer. Although beyond the scope of this paper, functional groups and the relative concentration[e] of these organic and inorganic compounds are essential for understanding the effect of dosing levels and their contamination mechanisms in fuel cells. This work focuses on the combined effect of all species present in each leachate solution on fuel cell performance.

Figure 2 shows, as an example of an in situ experiment, the iR-corrected cell voltage and high frequency resistance (HFR) response of a 50 cm^2 single cell, due to the contamination of one leachate solution from the 2-part adhesive category (Bond-IT B45). At 3.5 h, the infusion of the leachate solution started. Soon thereafter, the cell voltage dramatically decreased. This decline in performance slowed down at approximately 7 h and the cell reached a steady state poisoning state at approximately 15 h. The total performance loss at this point of the experiment was about 560 mV, i.e. from 0.78 V to 0.22 V. Subsequent to reaching a steady state poisoning state, the self-induced recovery started at 21.1 h. However, in this particular contamination case, no self-induced recovery of the cell performance was observed. After approximately 26.3 h the infusion experiment was stopped.

In the literature, three major contamination effects have been identified:[25–28] (i) a kinetic effect caused by adsorption of contaminant species on the electrode catalyst; (ii) an ohmic effect caused by

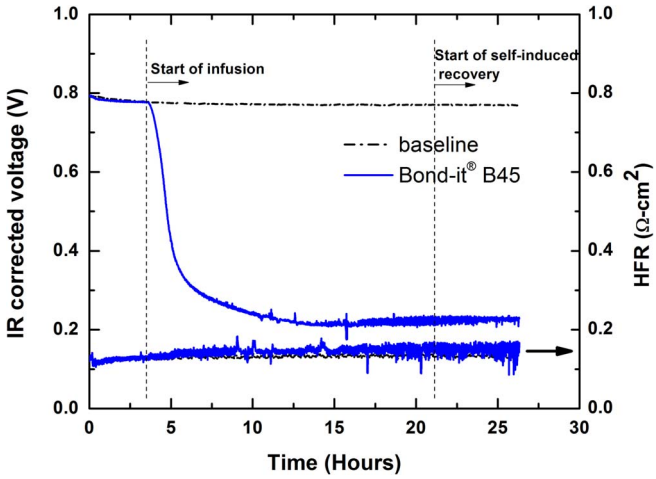

Figure 2. Comparison of iR-corrected voltage and HFR response due to infusion of DI water (baseline) and leachate solution from Bond-IT B45 material (1 week soak, 2-part adhesive family). Operating conditions were IEOC.

[e]We specify relative concentration because we were unable to quantify the concentrations of all constituent species.

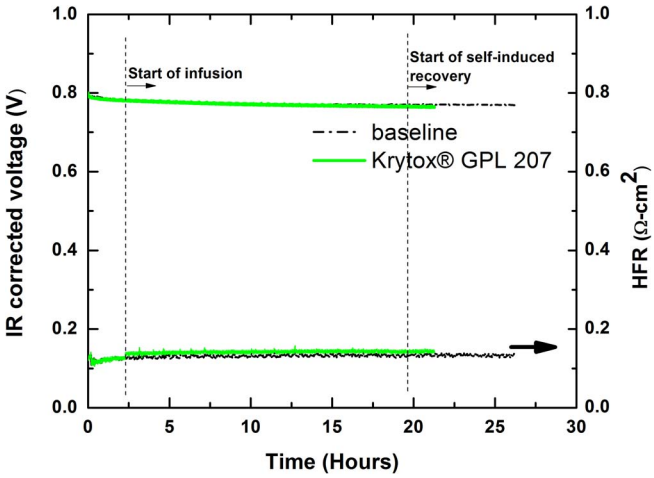

Figure 3. Comparison of iR-corrected voltage and HFR response due to infusion of DI water (baseline) and leachate solution from Krytox GPL 207 material (6 week soak, PFAE/PTFE greases family). Operating conditions were IEOC.

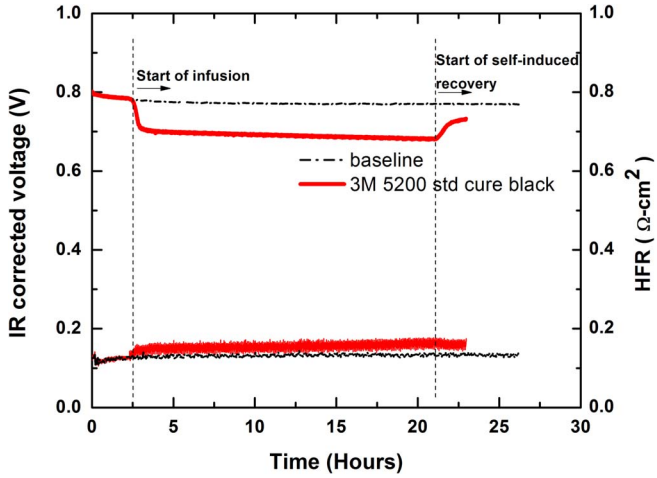

Figure 4. Comparison of iR-corrected voltage and HFR response due to infusion of DI water (baseline) and leachate solution from 3M 5200 standard cure black material (1 week soak, urethane adhesive/seal family). Operating conditions were IEOC.

reaction and/or absorption of contaminant species in both the ionomer of the catalyst layers and the membrane; and (iii) a mass transfer effect caused by a change of the catalyst layer structure and its hydrophobicity. In the data presented in Figure 2, the iR-corrected voltage is plotted vs. time. This entails that the performance losses due to the measured HFR, i.e. changes in the membrane resistance and contact resistances, were computed using Ohm's law and added to the actual measured performance data. Thus, any contamination effect that changes the membrane conductivity will not be visible as a performance decrease in Figure 2. Furthermore, the HFR does not increase substantially during this experiment. This may indicate that either the contaminant dosage, i.e., moles of contaminant = (moles/hour) ∗ (hour of exposure), was relatively small compared to the total amount of sulfonic acid groups in the membrane or that the contaminant does not significantly affect the conductivity of the electrolyte. Last but not least, we are operating the cell at low current density and low humidity for anode and cathode. At these conditions, the cell is not prone to flooding. The data shown in Figure 2 may therefore, allow one to conclude that the most likely contamination process in the cell is the kinetic effect (i) of contaminant adsorption on the Pt sites of the electrode catalyst.[29,30] The TOC value of this leachate solution was high (1695 ppm), while the total ICP count was low (3 ppm).[6] The results indicate that the organic compounds in the leachate solution may contain functional groups which are capable of adsorbing on the Pt surface and inhibiting the performance of the cell.

Figure 3 shows another example of the iR-corrected cell voltage and HFR response for the in situ infusion experiment using leachate solution created with a material from the PFAE/PTFE greases family (Krytox GPL 207). In this case, no apparent performance loss or HFR change was observed throughout the experiment. This may be related to the extremely low total ICP and TOC values, previously discussed with Figure 1, and/or the specific species present.

Figure 4 shows a third in situ example using leachate solution created with a material from the urethane adhesives/seals family (3M 5200 standard cure black). In this case, the contaminant was infused into the cathode at 2.5 h, and self-induced recovery was initiated at 21.2 h. The cell voltage response consisted of an immediate cell voltage loss of 88 mV, followed by a small steady decline, with respect to the baseline. As discussed in Figure 2, the rapid cell voltage response is likely associated with contaminant adsorption on the Pt surface. Compared to this main effect, the slower and smaller subsequent cell voltage decline may be associated with the HFR response, which shows a slow steady increase during contaminant exposure. One could speculate that either (i) the resistance of the catalyst layer is also increasing since this resistance is not included in the HFR, and thus is not being corrected for; or (ii) the correction for the measured HFR was slightly incomplete. The slight increase in HFR during contaminant exposure is likely due to absorption and/or reaction with the sulfonate sites in the membrane. However, the cell partially recovers from these effects when the contaminant is removed from the feed stream. In this case, cell voltage recovered by 51 mV within 1.85 h. The results indicate that some contaminant mechanisms are reversible at these operating conditions. While contamination in a fuel cell is not favorable, the ability to reverse contamination effects in a fuel cell system may be an important factor for BOP material selection.

In Figure 5, all of the iR-corrected voltage (a) and HFR changes (b), after infusion for 12 h, are plotted as a function of their TOC and total ICP values, respectively. The data suggest that there may be a weak correlation between the iR-corrected voltage loss and the TOC values. Several cases showed a performance loss below 50 mV, most cases had a performance loss between 50 –150 mV, and two cases had a performance loss of about 550 mV. In general, the data show that performance loss is likely to increase with increasing TOC values. However, the variation in the results may be related to the significant variety of organic molecules and functional groups in the leachate solutions. These include aliphatics, aromatics, polymerics, and amides, carboxylates, and alcohols, respectively, to name just a few.[17,21] All of these compounds may have specific contamination mechanisms associated with them, which may lead to varying performance losses. The investigation of individual compounds is beyond the scope of this paper, but reports of in situ and ex situ model compound studies have either been published or are underway.[21,31,32]

A stronger correlation may be apparent for the change of the HFR with increasing total ICP values. As shown in Figure 4, the HFR change as a function of time was not rapid. This time dependence may be directly related to the dosage of the inorganics that enter the membrane, which again should be directly correlated to the total ICP values. A worst-case scenario was calculated and is displayed in the last column of Table I. The calculation assumed that all the elements determined from ICP acted as Na^+ ions and they all exchanged sites with protons in the membrane. The result displayed in Table I is the minimum fraction of protons in the membrane available after infusion. This calculation showed that the inorganic cations present in the leachate solutions did not have enough exchange capacity to completely ion-exchange with the protons of the membrane. The actual observed change of the HFR for all cases was below 100 mΩcm^2 (Figure 5b), which may indicate that either (i) less ions were exchanged, or (ii) that an absorption process may have contributed to the loss in membrane conductivity. Note that organic cations may have also reacted with the sulfonic acid groups of the membrane. Similar to the performance/TOC data discussed above, the HFR/ICP data

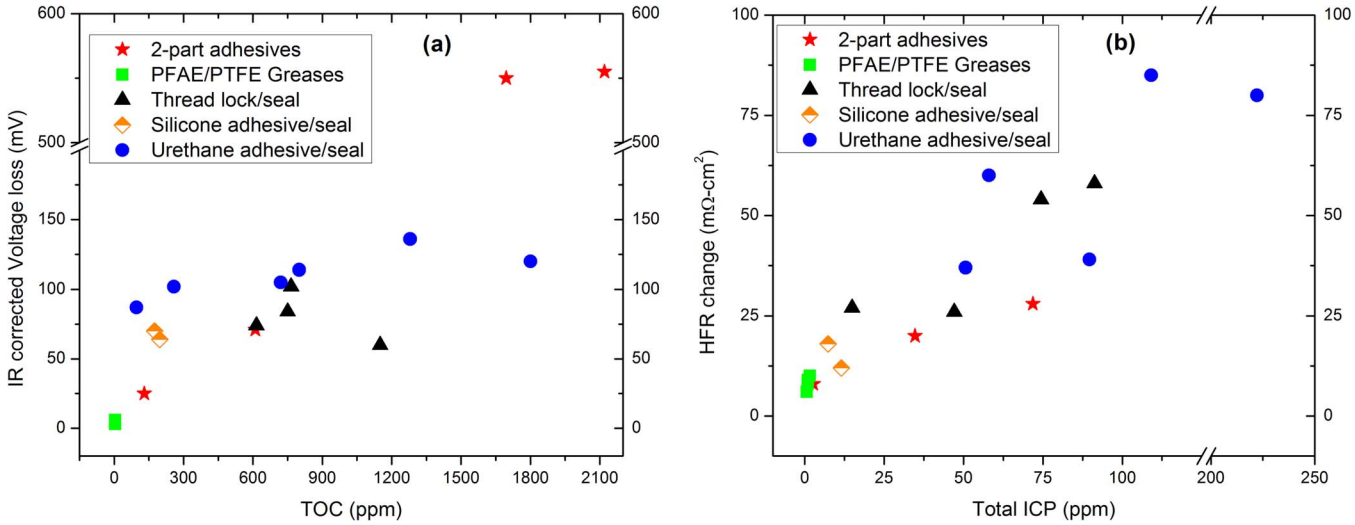

Figure 5. Relation between (a) iR-corrected voltage loss and TOC, (b) HFR change and total ICP after 12 hours of infusion with leachate contaminant from assembly aids materials. All materials were soaked for 1 week, except materials from the PFAE/PTFE greases family which were soaked for 6 weeks.

indicate that higher ICP values generally lead to a larger increase in HFR and consequently to a larger performance loss. Materials that resulted in leachate solutions with high total TOC and total ICP counts therefore have the potential to be more harmful to cell performance when used in a fuel cell system.

Figures 6, 7, and 8 compare data from BOT and EOT diagnostics for the infusion experiments discussed in Figures 2, 3, and 4, respectively. Figure 6 compares the fuel cell polarization curves obtained prior to the infusion experiment, i.e. labeled "Baseline", after the self-induced recovery phase, i.e. labeled "Post SI Recovery", and

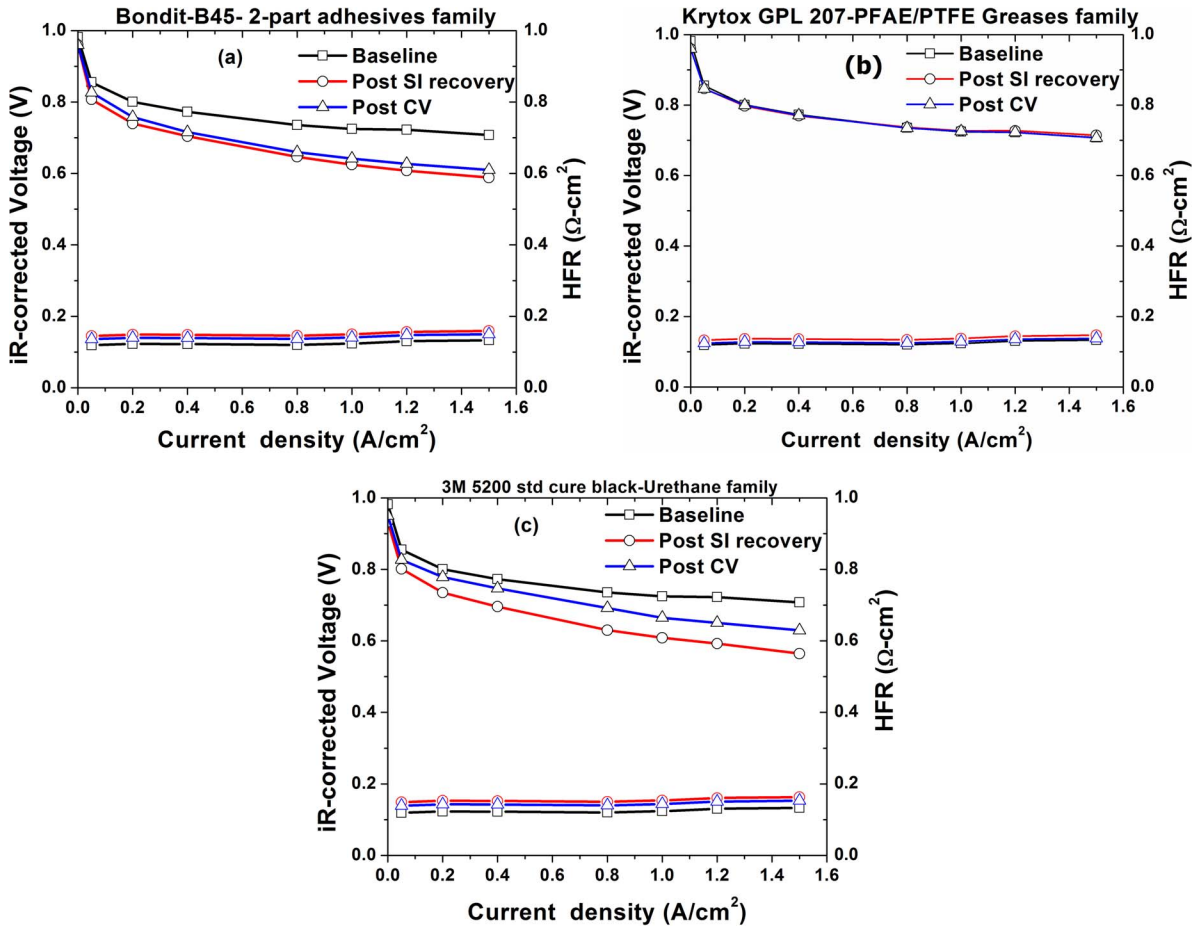

Figure 6. Comparison of BOT and EOT dry polarization curves: (□) prior to contaminant exposure, i.e., baseline, (○) post self-induced recovery: i.e. after contaminant infusion and then recovery without contaminant infusion, and (Δ) post CV measurements. (a) Bond-IT B45, (b) Krytox GPL-207, (c) 3M 5200 standard cure black. Operating conditions were dry and SOC.

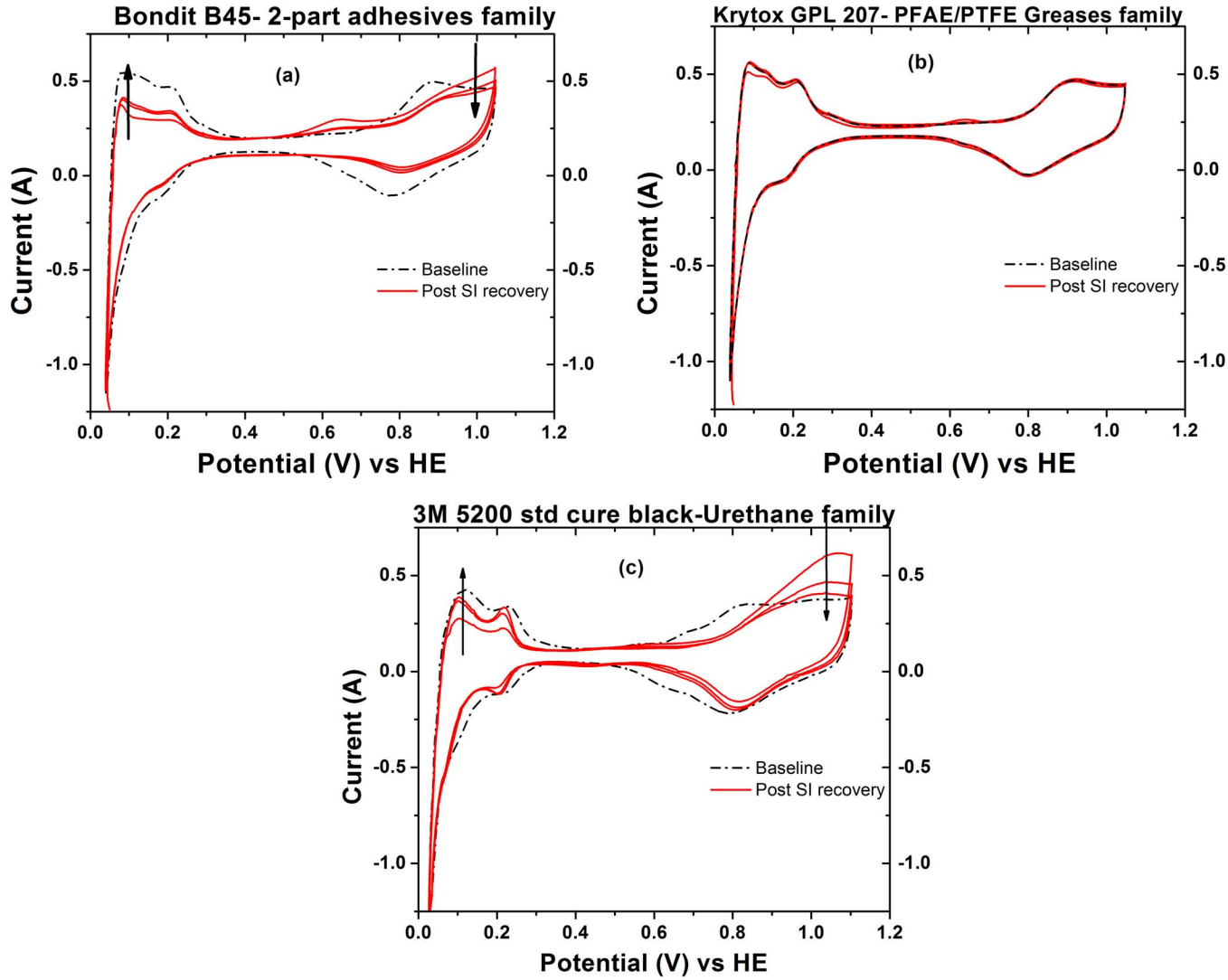

Figure 7. Comparison of the cathode CVs before (dash-dot) and after (solid) exposure to the assembly aids leachate: (a) Bond-IT B45, (b) Krytox GPL-207, (c) 3M 5200 standard cure black. CV measurements: Scan rate = 20 mV/s, RH% = 100/100, flow rate for H_2/N_2 = 200/100 sccm for anode/cathode, $T_{cell} = 80°C$. The arrows indicate progression with cycle number.

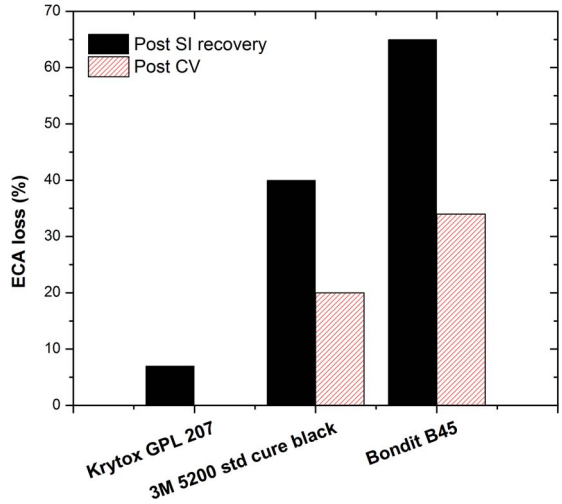

Figure 8. Percent ECA loss (compared to BOT ECA) after contaminant infusion and SI recovery [Post SI Recovery, solid bar] and after 3 potential cycles [Post CV, diagonal striped bar] for Krytox GPL-207, 3M 5200 standard cure black, and Bond-IT B45.

subsequent to driven recovery via CV, i.e. labeled "Post CV". All experiments were performed at SOC. The performance data for the cell exposed to the leachate solution from PFAE/PTFE greases (Figure 6b) show no apparent performance or HFR change, as may be expected from the infusion data shown in Figure 3. Figure 6b also shows that the data are reproducible. Similar data (not shown) was collected from an experiment during which DI-water was injected into the cell instead of contaminant leachate solution. No noticeable effects of the experimental procedure and methods were observed. The results of these reference experiments were identical to the results observed in Figure 6b, correlating that the very low contaminant levels of the PFAE/PTFE grease leachate solution have no effect on the fuel cell performance. More surprising was the performance comparison of the MEA exposed to the leachate solution from the 2-part adhesive Bond-IT B45 (Figure 6a). Despite a very strong performance decline of 560 mV during the infusion test (Figure 2), the performance curves of the initial performance (squares) vs. the performance after self-induced recovery (circles) differed by less than 70 mV at 0.2 A/cm^2. This is particularly interesting since no performance improvement had been observed during the self-induced recovery (Figure 2). This significant performance recovery observed via polarization curves (Figure 6a) may be due to the experimental procedure which involved shutting off the cathode gas flow, removing the nebulizer, and reconnecting

Table II. Percent ECA loss and polarization voltage loss (at 0.2 A/cm^2 during I-V measurement) determined after contaminant infusion and SI recovery and then after driven recovery.[10]

Materials family	Leachate solution	ECA loss after SI recovery (%)	ECA loss after CV recovery (%)	Voltage loss at 0.2 A/cm^2 after SI recovery (mV)	Voltage loss at 0.2 A/cm^2 after CV recovery (mV)
2-part adhesives	3M Scotch Weld1838 green	20	2	16	4
	LORD 204/19 extra thick acrylic	31	14	16	12
	Bond-IT B45	65	34	61	36
	Bond-IT B45TH	70	31	66	46
PFAE/PTFE greases	Krytox XHT-SX	7	0	11	8
	Krytox GPL-206	5	0	2	2
	Krytox GPL-207	7	0	6	2
	Krytox XHT-S	9	0	11	8
Thread lock/seal	Loctite #565	30	15	31	21
	Loctite #567	39	17	56	36
	Loctite #577	52	15	46	31
	Loctite #80724	20	12	26	16
Silicone adhesive/seal	3M #8663 clear	23	8	36	18
	3M #8664 black	15	5	16	11
Urethane adhesive/seal	Bostik 920 Fast set	40	18	72	26
	Loctite #39916	66	22	87	46
	3M 5200 standard cure black	40	20	66	46
	3M 5200 fast cure white	43	25	86	46
	3M 4000 fast cure white	50	23	57	31
	3M 5200 standard cure white	49	18	106	76

the standard gas lines and humidifier. During these steps the cell was exposed to open circuit potential, which may have had a mitigating effect for certain contaminant species.

Further improvement of the performance was accomplished by conducting the driven recovery via cyclic voltammetry (CV). The performance drop between the initial performance curve (Baseline, squares) and the performance after recovery via CV (Post CV, triangles) was reduced to less than 40 mV at 0.2 A/cm^2. This was commonly observed during this study. Voltammetric cycling typically resulted in an additional performance improvement for the leachates studied. A comprehensive list of the performance impacts (Post SI recovery and Post CV vs. Baseline) at a current density of 0.2 A/cm^2 is given in Table II, columns 5 and 6. As shown in Figures 7a and 7c, cycling to high potential appears to aid the recovery of the catalyst by oxidizing the organic contaminants. The baseline CV marked by dashed line shows features typical for a clean Pt electrode.[33] Note that the baseline CVs of the MEAs may slightly differ from each other, despite using identical MEAs from the same batch, and pretreatment and experimental procedures. To allow for accurate comparison of the CV responses, individual baseline CVs are required for each MEA. As expected, the CV after exposure to and SI recovery from the clean PFAE/PTFE family materials are the same as the baseline (Figure 7b). In contrast, the CVs during driven recovery (solid line) are very different from the BOT CV (dashed line) for both the Bond-IT B45 and 3M 5200 standard cure black materials (Figures 7a and 7c, respectively). The hydrogen adsorption/desorption peaks between 0.05 and 0.35 V and the Pt oxide reduction peak at 0.80 V are smaller compared to the baseline. This indicates a significant loss of active Pt sites. The arrows in the figure highlight the progression of the individual cycles. In the anodic scan of the first cycle, a peak is observed at approximately 0.65 V. This peak is likely related to contaminants in the leachate solution that can be removed from the catalyst via electro-oxidation.[34–37] The CVs also showed that the onset of Pt oxide formation has been delayed (shifted to higher potential) and perhaps some species is being oxidized (oxidation current at approximately 1 V is decreasing with cycling) during the anodic scans. This suggests that adsorbed contaminants from these leachates were oxidized and removed from the Pt surface during cycling. The removal of adsorbed species both contributed to the increase in the hydrogen desorption peak area with cycling. This increase, i.e. the removal of adsorbed species from the Pt sites, led to the slight improvement of cell performance between the "Post SI Recovery" and the "Post CV" cases shown in Figure 6a.

The data for the 3M 5200 standard cure black material from the urethane adhesives/seals family is shown in Figures 6c and 7c. The trend observed in the polarization data is similar to that for the 2-part adhesive Bond-IT B45. The worst performance was observed subsequent to infusion and self-induced recovery, and additional performance was recovered via potential cycling. In contrast to the Bond-IT B45 experiments however, the performance at the end of the 3M 5200 standard cure black infusion experiment was more similar to the performance observed during the polarization experiment. Thus, comparison of the performance data at 0.2 A/cm^2 to the infusion experiment appears to be more intuitive, although they were performed at slightly different operating conditions. The performance deviation between "Baseline" case and "Post SI Recovery" as well as "Post CV" case increased with increasing current density. This may be expected since the kinetic performance of the catalyst layer is inhibited when contaminant species adsorb on the catalyst surface.[23] Interestingly, while the performance drop during the infusion experiment was much smaller for the 3M 5200 standard cure black (perhaps related to the lower TOC values) compared to the Bond-IT B45, its performance drop during the polarization experiment was stronger. In addition, the CVs shown in Figure 7a and Figure 7c are fairly similar. This may strengthen the hypothesis that organic species adsorb onto Pt catalysts and an additional recovery process may have occurred during the Bond-IT B45 experiment.

Figure 8 summarizes the loss of electrochemically active Pt surface area after self-induced recovery and after performing recovery CVs for the three example material cases discussed above. The post SI recovery data was determined from partial CVs and the post CV data from full potential CVs as shown in Figure 9. For all three cases, catalyst surface sites were lost due to adsorption of species on the surface. Note that a typical variation of ECA data is ±5%. In any case, the data indicate that the higher the TOC of the leachate solution, the higher the observed loss of surface area. Quantitative ECA values for all twenty material leachates studied are listed in Table II. For all of the three materials shown in Figure 8, the driven recovery

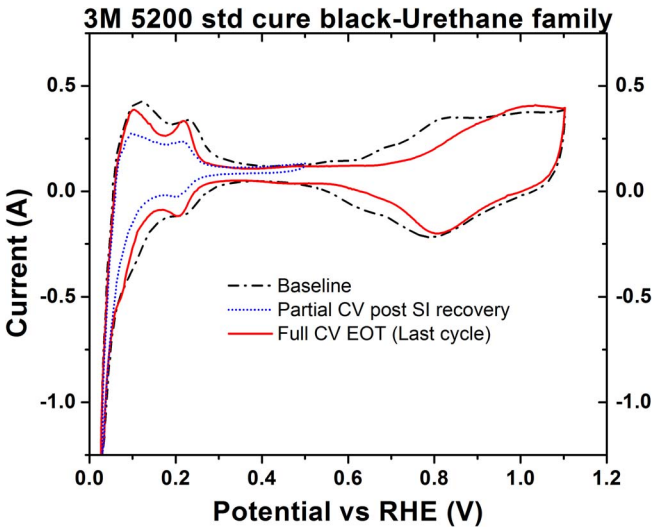

Figure 9. Comparing cathode CV data obtained at various times throughout an infusion experiment with 3M 5200 standard cure black leachate solution. The baseline full CV was obtained at BOT (dash-dot), the partial CV (dot) was obtained after SI recovery, and the second full CV (solid) was obtained after the EOT polarization measurement. Scan rate = 20 mV/s, RH = 100%/100%, flow rate for H_2/N_2 = 200/100 sccm for anode/cathode, T_{cell} = 80°C.

via CV removed adsorbed surface species from the Pt catalyst. The performance improvement due to this recovery is apparent in the performance increases shown in Figure 6. The extent of recovery however, was different. For Krytox GPL 207, 3M 5200 standard cure black, and Bond-IT B45, the percentage of recovered sites from the lost Pt sites were 100%, 50%, and 48%, respectively.

As indicated by the values given in Table II, the % ECA recovery does not transfer 1:1 into performance recovery. For example, a 50% ECA recovery resulted in a 30% performance recovery for the 3M 5200 standard cure black material. This may be related to the observed changes in the CVs apparent in Figure 7. Using the 3M material as an example, the third and final cycle of the CV showed significant deviation from its baseline CV. The hydrogen adsorption and desorption peaks are less pronounced and the onset for Pt oxide formation has shifted to higher potentials. These changes in conjunction with potentially increased catalyst layer resistance likely have contributed to the overall performance change observed in Figure 6.

Conclusions

In this study the effects of fuel cell exposure to balance of plant materials were investigated. The study included accelerated aging of twenty assembly aids materials that covered a wide range of functions and properties. It is reasonable to assume that the concentrations of contaminants in the leachate solutions are higher than expected in a fuel cell system. The studied leachate solutions resulted in a variety of performance and recovery effects, which were characterized using in situ performance, constant current, and cyclic voltammetry experiments. Complementary ex situ experiments performed included TOC and ICP. The effects can be used to classify BOP materials into categories. Such classification may include but is not limited to:

Classification	Performance Impact	Self-induced Recovery	Driven Recovery
(i)	None	N/A	N/A
(ii)	Yes	Complete	N/A
(iii)	Yes	Partial	Complete
(iv)	Yes	None	Complete
(v)	Yes	Partial	Partial
(vi)	Yes	None	Partial
(vii)	Yes	None	None

The three example data sets discussed above would consequently fall into categories (vi), (i), and (v) for Bond-IT B45, Krytox GPL207, and 3M 5200 standard cure black, respectively.

Generally the performance impact scaled with TOC values of the created solutions, and the observed HFR change scaled with total ICP values. The data indicated three different types of impact: (i) adsorption of contaminant species on the Pt catalyst, (ii) absorption in the membrane or reaction with the sulfonate sites in the membrane, and (iii) absorption in the ionomer of the catalyst layer or reaction with the sulfonate sites in the ionomer of the catalyst layer.

The presented study focused on investigating the effects of a mixture of organic, inorganic and ionic contamination, i.e. the total sum of compounds entering the DI water during the leaching process. However, individual compounds with specific functional groups may have contributed stronger to the observed effects. To further understand the effect of individual functional groups that may carry the most weight in poisoning the fuel cell, model compound studies are required. Such studies may help to determine any correlation between the functional groups of the organic/inorganic compounds, found in GCMS/ICP/ion chromatography, with adsorption on the catalyst. They would thus help to identify which species impact ECA and/or ionomer conductivity. Future work will address identifying such compounds and functional groups to support the industry in their BOP material selection. Such knowledge may also be useful to identify or design new material sets that are suitable for fuel cell applications.

Acknowledgment

The authors gratefully acknowledge support for this work by the DOE EERE Fuel Cell Technologies Office (DE-AC36-08GO28308) under a subcontract from NREL (ZGB-0-99180-1) to the University of South Carolina. We thank Dr. Christ and Dr. Ranville's analytical lab from Colorado School of Mines for providing ICP-OES data and Dr. Wang from NREL for providing TOC data. We would further like to thank our collaborating partners at General Motors for providing assembly aids materials and for valuable discussions and guidance.

Appendix

In this section we present an example calculation for determining the minimum membrane protonic fraction after complete ion-exchange reaction with species identified by ICP (assumed to be sodium cation). Example leachate solution is Bond-IT B45TH. Results for all leachate solutions are given in Table I.

The membrane material of the MEAs was Nafion 211 which has an acid capacity of 0.95 mmol/g.

50 cm^2 of this MEA contains 268 μmol sulfonic acid sites.

The leachate solution of Bond-IT B45TH has ≈ 72 ppm ICP total cations (See Table I).

For the calculation we assume that all the cations act as sodium ions. We also assume that all of them ion-exchange with protons in the Nafion 211 membrane.

The leachate is infused over a course of 12 hours at a flow rate of 0.03 cc/min.

The total dosage of cations infused is thus 68 μmol.

Assuming a charge of 1 for each cation, the fraction of protons remaining in the membrane after infusion is then:

$$\frac{(Total\ acid\ capacity\ of\ membrane - (cation\ dosage * cation\ charge))}{Total\ acid\ capacity\ of\ membrane} = 0.76$$

References

1. M. Das, M. Ohashi, C. S. Macomber, H. Wang, H. Dinh, K. A. O'Leary, R. Reid, B. Lakshmanan, and J. Van Zee, *Presented at the 220th Meeting of the Electrochemical Society*, Boston, MA, on Oct. 12, 2011. ECS Abstract #1039.
2. Q. Guo, R. Pollard, and J. Ruby, *ECS Transactions*, **5**, 187 (2007).
3. B. D. James and A. B. Spisak, *Mass Production Cost Estimation of Direct H2 PEM Fuel Cell Systems for Transportation Applications: 2012 Update* (2012).
4. B. Lakshmanan, K. O'Leary, and R. Reid, in *Meeting Abstracts*, p. 1638 (2012).
5. C. Macomber, H. Wang, K. O'Neill, S. Coombs, G. Bender, B. Pivovar, and H. N. Dinh, *ECS Transactions*, **33**, 1637 (2010).
6. C. S. Macomber, J. Christ, H. Wang, B. S. Pivovar, and H. N. Dinh, *ECS Transactions*, **50**, 603 (2013).
7. C. S. Macomber, H. Wang, K. O'Neill, J. Christ, M. Das, J. Van Zee, K. A. O'Leary, and H. Dinh, *Presented at the 220th Meeting of the Electrochemical Society*, Boston, MA, on Oct. 12, 2011. ECS Abstract #1040.

8. K. O'Leary, B. Lakshmanan, and M. Budinski, 2009 Canada-USA PEM Network Research Workshop, February 16 (2009).
9. K. A. O'Leary, R. Reid, and B. Lakshmanan, *Presented at the 220th Meeting of the Electrochemical Society*, Boston, MA, on Oct. 12, 2011. ECS Abstract #1036.
10. M. S. Opu, M. Ohashi, H.-S. Cho, C. S. Macomber, H. N. Dinh, and J. W. Van Zee, *ECS Transactions*, **50**, 619 (2013).
11. M. Uchimura, S. Sugawara, Y. Suzuki, J. Zhang, and S. S. Kocha, *ECS Transactions*, **16**, 225 (2008).
12. H. Wang, S. Coombs, C. Macomber, K. O'Neill, G. Bender, B. Pivovar, and H. N. Dinh, *ECS Transactions*, **33**, 1617 (2010).
13. E. F. Holby, Y. Shao-Horn, W. Sheng, and D. Morgan, *ECS Transactions*, **25**, 583 (2009).
14. S. Lee, D. Bessarabov, and R. Vohra, *International Journal of Green Energy*, **6**, 594 (2009).
15. A. A.-M. Marcu, G. Toth, and P. Pietrasz, *ECS Transactions*, **50**, 1523 (2013).
16. K. G. Budinski and M. K. Budinski, p. 768, Prentice Hall, NJ (2005).
17. H.-S. Cho, M. Jung, J. Navarro, M. Ohashi, and J. W. Van Zee, *ECS Transactions*, **33**, 1627 (2010).
18. G. A. James, S. M. Mackinnon, D. R. Sousa, D. A. Summers, W. M. Williams, J. Bellerive, M. L. Bos, R. B. P. Rempel, S. Farrington, and S. J. McDermid, "Prevention of membrane contamination in electrochemical fuel cells," in US Pat. Application US2005089746A.
19. R. Moses, in *National Research Council Canada Institute for Fuel Cell Innovation, International Fuel Cell Testing Workshop* (2006).
20. J. St-Pierre, in *Polymer Electrolyte Fuel Cell Durability*, p. 289, Springer (2009).
21. http://www.hydrogen.energy.gov/pdfs/review13/fc048_dinh_2013_o.pdf.
22. http://www.nrel.gov/hydrogen/contaminants.html.
23. H. Wang, C. Macomber, J. Christ, G. Bender, B. Pivovar, and H. N. Dinh, *Electrocatalysis*, **5**, 62 (2014).
24. P. T. Yu, E. A. Bonn, and B. Lakshmanan, *ECS Transactions*, **58**, 665 (2013).
25. A. Collier, H. Wang, X. Zi Yuan, J. Zhang, and D. P. Wilkinson, *International Journal of Hydrogen Energy*, **31**, 1838 (2006).
26. S. Knights, N. Jia, C. Chuy, and J. Zhang, Palm Springs, California (2005).
27. J. St-Pierre, D. Wilkinsor, S. Knights, and M. Bos, *Journal of New Materials for Electrochemical Systems*, **3**, 99 (2000).
28. J. Zhang, H. Wang, D. P. Wilkinson, D. Song, J. Shen, and Z.-S. Liu, *Journal of Power Sources*, **147**, 58 (2005).
29. X. Cheng, Z. Shi, N. Glass, L. Zhang, J. Zhang, D. Song, Z.-S. Liu, H. Wang, and J. Shen, *Journal of Power Sources*, **165**, 739 (2007).
30. H.-S. Cho, M. S. Opu, M. Ohashi, and J. Van Zee, *Presented at the 222nd Meeting of the Electrochemical Society*, Honolulu, HI, on Oct. 9, 2012. ECS Abstract #1295.
31. J. M. Christ, K. Neyerlin, R. Richards, and H. N. Dinh, *Journal of The Electrochemical Society*, **161**, F1360 (2014).
32. J. M. Christ, K. Neyerlin, H. Wang, R. Richards, and H. N. Dinh, *Journal of The Electrochemical Society*, **161**, F1481 (2014).
33. H. A. Gasteiger, S. S. Kocha, B. Sompalli, and F. T. Wagner, *Applied Catalysis B: Environmental*, **56**, 9 (2005).
34. M. Angelo, G. Bender, S. Dorn, K. Bethune, T. Hossain, D. Posey, J. Gazda, A. Ghatak-roy, and R. Rocheleau, *ECS Transactions*, **16**, 669 (2008).
35. G. Bender, M. Angelo, K. Bethune, and R. Rocheleau, *Journal of Power Sources*, **228**, 159 (2013).
36. G. Bender and T. A. Zawodzinski, in *Proceedings of the Electrochemical Society*, p. 31 (2002).
37. S. Dorn, G. Bender, K. Bethune, M. Angelo, and R. Rocheleau, *ECS Transactions*, **16**, 659 (2008).